Progress In Electromagnetics Research C, Vol. 24, 111–122, 2011

SELF-COMPLEMENTARY CIRCULAR DISK ANTENNA FOR UWB APPLICATIONS

K. H. Sayidmarie[1,*] and Y. A. Fadhel[2]

[1]College of Electronic Engineering, University of Mosul, Iraq

[2]Department of Electronic Techniques, Institute of Technology, Mosul, Iraq

Abstract—In this paper, the self-complementary principle has been applied to develop the traditional planar monopole antenna into a dipole antenna whose frequency range exceeds UWB requirements. The proposed design has compact, planar, and simple shape arranged in self-complementary manner connected to the (SMA) connector via rectangular microstrip line. The self-complementary structure offers better reduction of the imaginary part of antenna impedance, which allows matching on a wider band of frequencies. The proposed antenna showed -10 dB return loss bandwidth extending from 1.86 GHz up to 17.7 GHz. Moreover, this antenna has a simple shape as compared with complicated and irregular shapes with curves, slots or parasitic elements. The proposed design is validated by experimental measurements. The phase of the return loss is investigated for more insight into antenna matching.

1. INTRODUCTION

The last decade has witnessed significant research activities in the field of ultra wideband (UWB) antennas. A large number of antenna configurations offering UWB characteristics have been proposed and investigated [1–5]. Among the proposed shapes are a planar volcano-smoke slot antenna [1, 2], triangular monopole [3], circular and elliptical disc monopoles [5, 6]. The dipole configuration has also been investigated for the UWB required characteristics, where square, triangular, circular, and other shapes for the two arms have been used [7, 8]. Most of the adopted design methodologies were trial and error methods with the help of a simulation tool to get the desired

Received 25 July 2011, Accepted 7 September 2011, Scheduled 10 September 2011

* Corresponding author: Khalil Hassan Sayidmarie (kh.sayidmarie@gmail.com).

UWB operation by tailoring corners, tips, slots, or parasitic parts. Other designs used optimization techniques such as Particle Swarm Optimization (PSO) procedure [9], where the dimensions and shape of a monopole are optimized. Some of the achieved antenna designs have very complicated geometries that are sensitive to the manufacturing tolerances when implemented practically. Nevertheless, there are some other methods that can be exploited to design efficient UWB antennas, but unfortunately, these methods are rarely used. One of these methods is to use the principle introduced by Yasuto Mushiake in the 1940s to account for so-called self-complementary antennas. He found that *the product of input impedance of a planar electric current antenna (patch) and its corresponding 'magnetic current' antenna (slot) is a real constant.* Therefore, an antenna built in a complementary structure of electric and magnetic currents exhibits a real constant impedance [10]. There were some attempts by some researchers to apply this technique for designing UWB antennas with a good impedance bandwidth, as that by Lu Guo et al. [11]. However, the efforts were made in performing miniaturization rather than enhancing the impedance bandwidth.

In this paper, the self-complementary principle is applied to the design of UWB dipoles where the two arms of the dipole antenna are made in the form of circular disc and slot. For this purpose, we start with conventional circular monopole with ground plane antenna. The feed line is then modified from the conventional geometry to another one that is suitable for the proposed configuration of self-complementary dipole antenna. The proposed design is investigated by computer simulations using CST Microwave Studio^{TM} package which utilizes the Finite Integration Technique for electromagnetic computation. Validity of the proposed design was confirmed by experimental measurements.

2. ANTENNA DESIGN

2.1. Circular Monopole Antenna with Straight Microstrip Feed Line — Antenna (i).

The first configuration of the UWB antennas, which have been investigated here, is the circular disc monopole shown in Figure 1(a). It is interesting to examine the operation principle of planar UWB monopoles and why this resonating type of antenna has almost omnidirectional pattern. For the disc monopole, it is difficult to identify the resonance modes of the antenna on the Smith chart in the traditional way, where reactance equal to zero and resistance equal to 50 Ohm are the criteria. However, dips in the return loss curve,

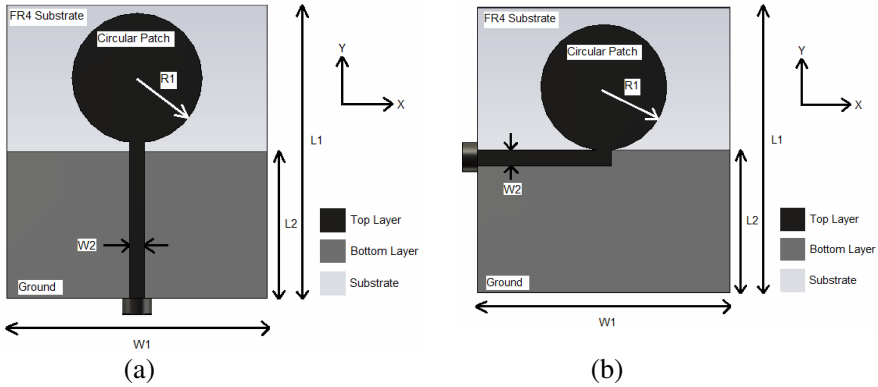

Figure 1. Geometry of circular monopole antennas: (a) antenna (i) with straight feed line, (b) antenna (ii) with bended feed line.

Table 1. Comparison of design parameters and obtained frequency characteristics of the three designed antennas.

Parameter	*Antenna (i)*	*Antenna (ii)*	*Antenna (iii)*
L_1 [mm]	52	52	52
L_2 [mm]	26	26	26
W_1 [mm]	46	46	46
W_2 [mm]	2.6	2.8	2.8
R_1 [mm]	11.5	11.5	11.5
R_2 [mm]	-	-	11.5
Metalization Thickness [mm]	0.035	0.035	0.035
$f_{\min}$ [GHz]	1.63	5.014	1.86
$f_{\max}$ [GHz]	12.2	11.5	17.77
BW [GHz]	10.57	6.486	15.91
$f_{\max}/f_{\min}$	7.48:1	2.29:1	9.55:1

which indicate better impedance matching at certain frequencies, can be regarded as the resonances of the antenna. The first resonant frequency is determined by the diameter of the disc where it is about 0.25 of the wavelength in air [5]. An account for the feed-gap length and the relative dielectric constant of the substrate was given in [12], which slightly reduces the above factor. The rest of resonances seem to be the harmonics of the first one as the other current modes on the disc will arrange themselves in an integer multiple fashion of the lowest mode. Thus the overlapping of closely spaced multiple resonances leads

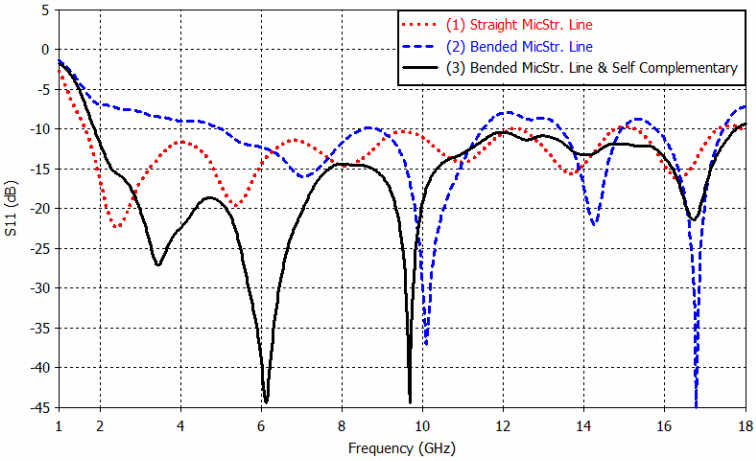

Figure 2. Return loss curves for the three designed antennas.

to the wanted UWB features.

For microstrip fed disc monopole, the copper radiator and 50 Ω feed line are printed on the same side of the dielectric substrate, while the ground plane is printed on the other side of the substrate, as illustrated in Figure 1(a). The geometry illustrated in Figure 1(a) was simulated assuming a dielectric FR4 substrate of 1.6 mm thickness, relative permittivity of 4.3, and dielectric loss tangent of 0.025. The design parameters were: disc radius $R_1 = 11.5$ mm and microstrip feed line width $W_2 = 2.6$ mm. Other design parameters and the resultant frequency characteristics are shown in the 2nd column of Table 1.

Figure 2 shows the return loss curve in red dotted line obtained from the simulation. As can be seen from Figure 2 and Table 1, the obtained (VSWR < 2) frequency range extends from 1.63 to 12.2 GHz, which forms a 7.48 to 1 bandwidth ratio. The input impedance is shown on the Smith chart of Figure 3(a). On the chart, the points nearest to the center (nearest to matching) have been marked on the zoomed VSWR = 2 circle. These points occur at frequencies of (2.43, 5.36, 8.06, 10.99, 13.66, 16.34) GHz, which correspond to the six dips in return loss pattern shown in Figure 2. The radiation patterns in the three principal planes are plotted in Figure 4, for selected frequencies of (3, 5, 7.5 & 10) GHz.

2.2. Circular Monopole Antenna with Bended Microstrip Feed Line — Antenna (ii).

The feed line of the previous monopole was then modified to the geometry shown in Figure 1(b), where the microstrip line has been

bended by 90°. In this configuration, the feed line runs parallel to the edge of the ground plane. The design parameters and obtained frequency characteristics are also listed in the 3rd column of Table 1. Figure 2 shows the obtained return loss curve in blue dashed line compared to that of the straight feed line monopole. The obtained (VSWR < 2) frequency range extends from 5.014 to 11.5 GHz, leading to 2.29 to 1 bandwidth ratio. It can be seen that some part of the lower UWB range has been lost. The variation of input impedance is shown on the Smith chart of Figure 3(b). On the chart, the points nearest to the center (nearest to matching) have also been marked on the zoomed VSWR $= 2$ circle. These points occur at frequencies of (7.08, 10.1, 14.24, 16.78) GHz, which correspond to the four dips in return loss pattern shown in Figure 2. No further optimization was made on this design as this arrangement is prepared for the other design which will

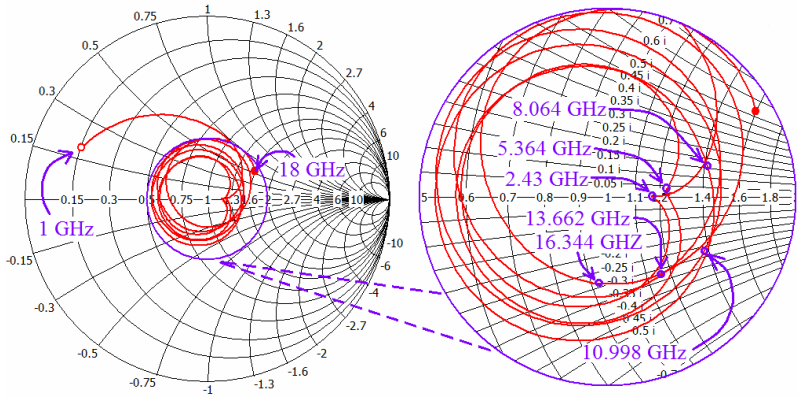

(a)

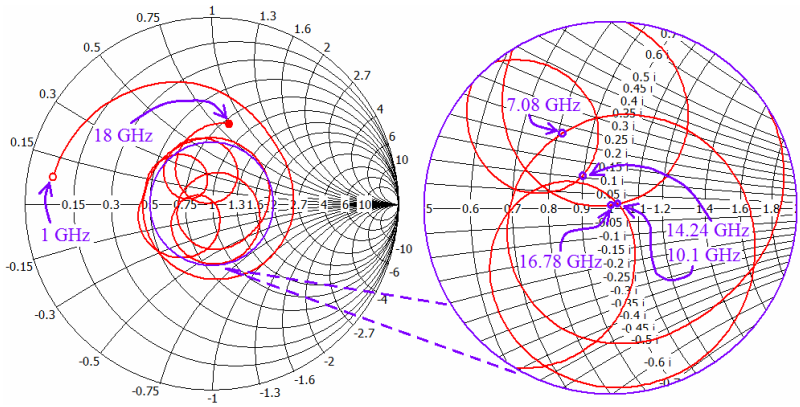

(b)

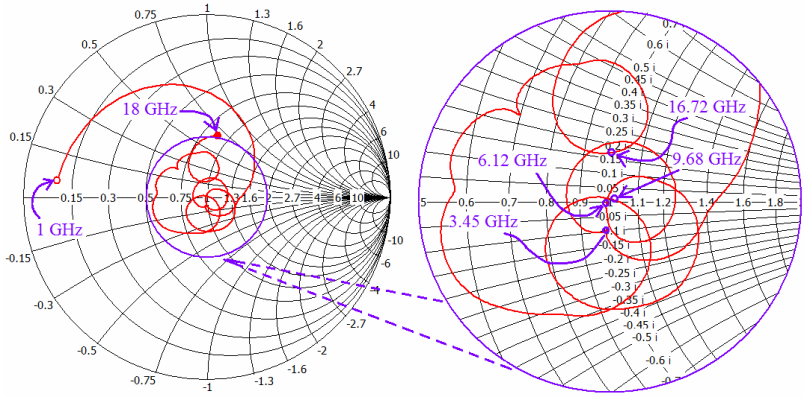

(c)

Figure 3. Smith charts for (a) antenna (i), (b) antenna (ii), (c) antenna (iii), showing zoomed (VSWR = 2) circle on the right.

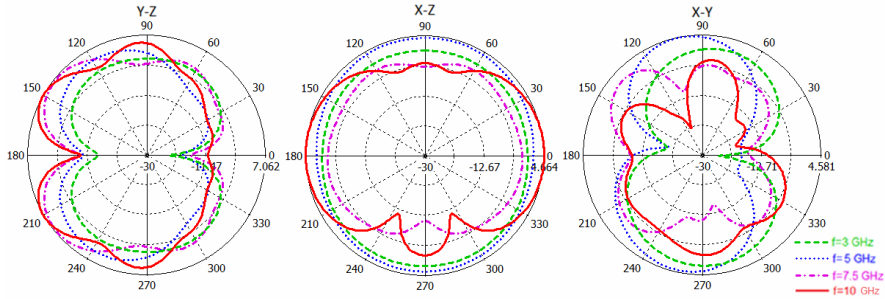

Figure 4. Radiation patterns in the three principal planes for antenna (i).

be discussed in the next Section 2.3. The radiation patterns in the three principal planes are plotted in Figure 5, for selected frequencies of (3, 5, 7.5 & 10) GHz. In comparison with the results of Figure 4 (for antenna (i)), the patterns in YZ-plane (E-plane), and XZ-plane (H-plane) show some changes, while the XY-plane shows some improvement, but it is still not omnidirectional.

2.3. Self-complementary Circular Dipole Antenna with Bended Microstrip Line Feed — Antenna (iii)

With the self-complementary principle in mind, the proposed antenna configuration was developed by the procedure shown diagrammatically in Figure 6. In this configuration, the rectangular copper plane works

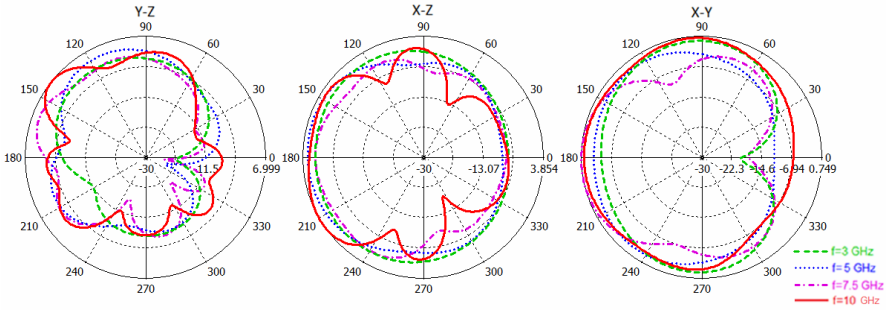

Figure 5. Radiation patterns in the three principal planes for antenna (ii).

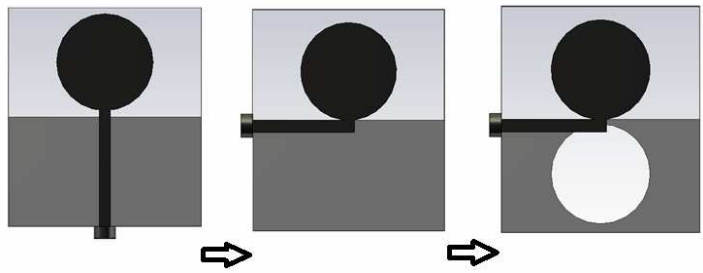

Figure 6. Development procedure for the microstrip fed self-complementary dipole antenna.

as ground plane for the disc arm and slot arm of the dipole, as well as for the microstrip feed line. The bending of the feed line offers the possibility of feeding the dipole at its center. Direct connection to one arm and aperture coupling to the slot arm are provided by this arrangement.

Figure 7 shows detailed design and parameters of the proposed self-complementary dipole antenna. The parameter values of the designed antenna are listed in the 4th column of Table 1. The return loss curve of the simulated antenna is plotted in Figure 2, where it can be seen that the return loss of self complementary antenna is better than those of the previous monopoles. The (VSWR < 2) bandwidth extends from 1.86 to 17.77 GHz giving a bandwidth ratio of 9.55:1. The input impedance performance is shown in Figure 3(c). The chart shows the points nearest to the center (nearest to matching) as marked on the zoomed VSWR $= 2$ circle. These points occur at frequencies of (3.45, 6.12, 9.68, 16.72) GHz, which correspond to the four dips

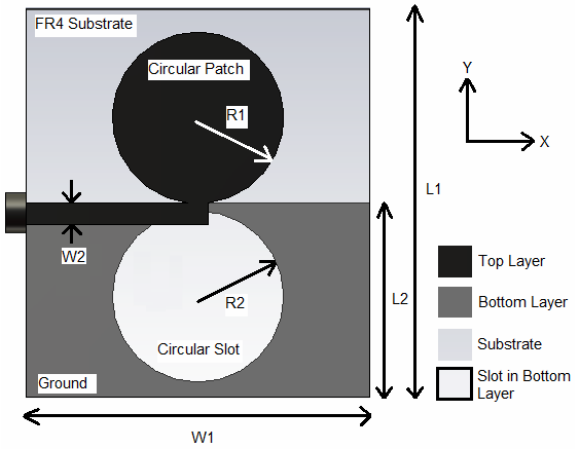

Figure 7. Geometry of the proposed self-complementary dipole antenna of circular shape — antenna (iii).

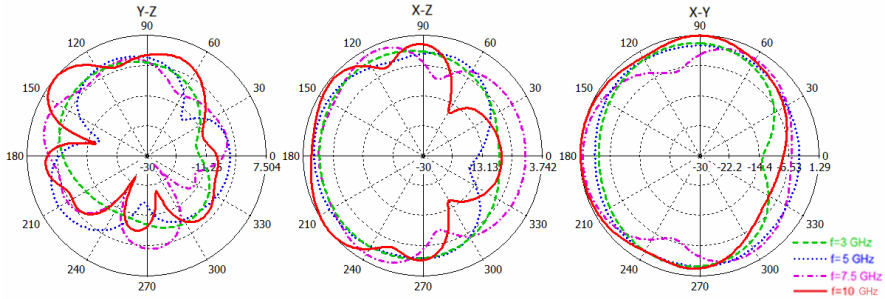

Figure 8. Radiation patterns in the three principal planes for antenna (iii).

in return pattern shown in Figure 2. The radiation patterns in the three principal planes are plotted in Figure 8, for selected frequencies of (3, 5, 7.5 & 10) GHz. In this antenna very wideband operation has been observed, which covers and exceeds the UWB range, while good radiation pattern approaching omnidirectional shape is maintained.

The gain and radiation efficiency have been calculated using the results of simulations of antenna (iii) as shown in Figure 9. The efficiency is seen decreasing with frequency due to losses, while the gain increases for frequencies up to about 10 GHz then starts to drop slightly. Therefore, the return loss, radiation pattern, gain, and radiation efficiency are all important parameters that specify the performance of an antenna.

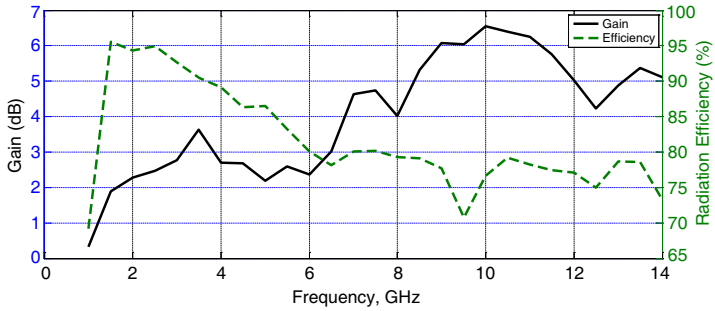

Figure 9. Calculated gain and efficiency for antenna (iii).

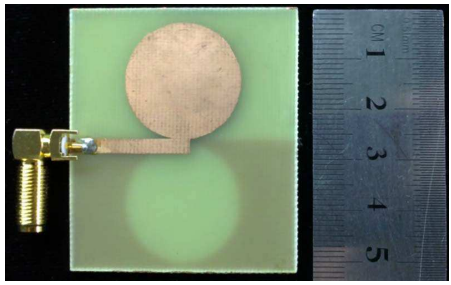

Figure 10. Photograph showing the fabricated self-complementary dipole antenna (iii).

3. EXPERIMENTAL RESULTS

The verification of simulated results for the antenna is presented here with the experimental results. The self-complementary dipole antenna (iii), which was investigated in Section 2.3 by simulation, was fabricated using the same substrate and design parameters listed in column 4 of Table 1. A CNC PCB cutting machine was used in the fabrication, and the obtained antenna is shown in Figure 10. The Rode and Schwarz ZVL13 vector network analyzer (VNA) was used to measure the return loss over the frequency range of 1 GHz–13.6 GHz. The measured return loss S_{11} data set comprised 201 discrete data points in magnitude $|S_{11}|$ and phase $\arg(S_{11})$, which were exported to a USB memory through the VNA port.

The experimental results of the return loss of the self-complementary antenna and those obtained from the simulation are shown in Figure 11. It can be seen that the antenna is matched (return loss < -10 dB) across the frequency range which extends from

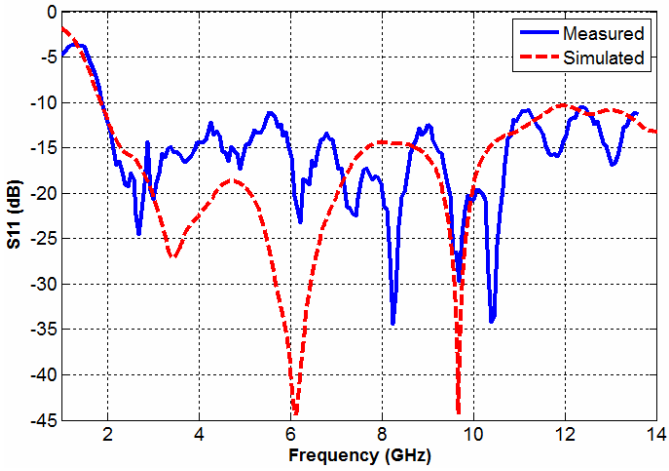

Figure 11. Measured and simulated return loss magnitude for the fabricated self-complementary dipole antenna (iii).

1.882 GHz, as compared to 1.86 GHz from the simulation, to above 13.6 GHz. The later value is the limit of the bandwidth of the network analyzer, thus it was not possible to examine the antenna beyond this value. The measured return loss curve shows 6 deep (below -20 dB) dips which are related to six frequencies at which the antenna is in near resonance. However, the simulated return loss result, which is also plotted in Figure 11 for comparison, shows 3 deeper dips for the same frequency range. Nevertheless, the experimental result complies with the criteria of less than -10 dB return loss over the range 1.882 to more than 13.6 GHz.

For further investigations, we propose to use the phase of the return loss curve which has been obtained from the recorded VNA measurements. Figure 12 shows the phase response after the measured phase has been unwrapped by adding 2π at each phase jump in the $\arg(S_{11})$ curve. The variation of the unwrapped phase with frequency $\Phi(f)$ shows mainly linear trend with relatively minor imposed fluctuations and can be represented by the following relation:

$$\Phi(f) = \Phi_0 + k(f - f_1) + \text{ higher order terms} \quad \text{for } f >= f_1 \qquad (1)$$

where Φ_0 is a constant; k is the phase slope in degrees/GHz; f and f_1 are frequencies in GHz. For the shown curve, it was found that $\Phi_0 = 212$ degree, $f_1 = 3.016$ GHz, and $k = 215$ degree/GHz give a good representation of the first two terms of Equation (1). After subtracting these two estimated terms, the resulting phase curve is shown (dotted)

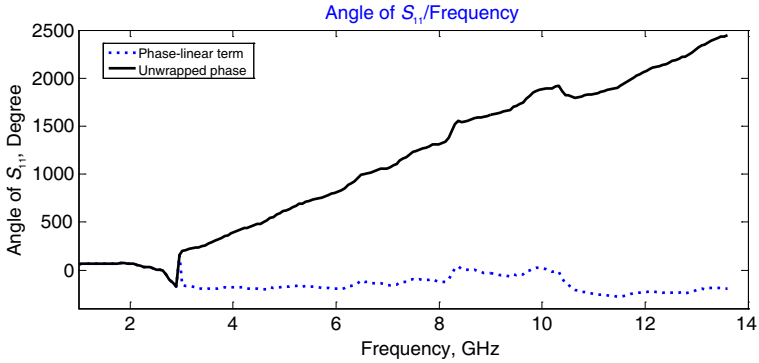

Figure 12. Variation of the return loss phase with frequency for the self-complementary dipole antenna (iii). (—) Unwrapped phase, (....) unwrapped phase after subtracting the linear term.

also in Figure 12. The phase changes are much more pronounced now, and they clearly mark the regions of the above mentioned resonances. Therefore, the phase curve can give more insight for the study of matching and return loss of the investigated antenna.

4. CONCLUSIONS

It has been demonstrated that self-complementary principle can be used in designing UWB dipole antennas. Simulation results show that bending of the conventional microstrip line feed of the printed disc monopole has a little impact on the radiation patterns, while some reduction in the bandwidth is noticed. The proposed self-complementary dipole antenna shows a return loss performance better than those of the conventional and bended feed line monopoles. Wider bandwidth has been achieved. The application of self-complementary principle is very promising technique that encourages design trends towards antennas with simpler shapes. The phase of the return loss curve can give more insight into the investigation of antenna matching.

REFERENCES

1. Yeo, J., Y. Lee, and R. Mittra, "Wideband slot antennas for wireless communications," *IEE Proc. Microwaves Antennas and Propagation*, Vol. 151, 351–355, 2004.

2. Ying, C., G. Li, and Y. Zhang, "An LTCC planar ultra-wideband antenna," *Microwave and Optical Technology Letters*, Vol. 42, 220–222, 2004.
3. Lin, C., Y. Kan, L. Kuo, and H. Chuang, "A planar triangular monopole antenna for UWB communication," *IEEE Microwave and Wireless Components Letters*, Vol. 15, No. 10, 624–626, 2005.
4. Lee, S., J. Park, and J. Lee, "A novel CPW-fed ultra-wideband antenna design," *Microwave and Optical Technology Letters*, Vol. 44, 393–396, 2005.
5. Liang, J., C. Chiau, X. Chen, and C. Parini, "Study of a printed circular disc monopole antenna for UWB systems," *IEEE Transactions on Antennas and Propagation*, Vol. 53, No. 11, 3500–3504, 2005.
6. Wang, L., W. Wu, X.-W. Shi, F. Wei, and Q. Huang, "Design of a novel monopole UWB antenna with a notched ground," *Progress In Electromagnetics Research C*, Vol. 5, 13–20, 2008.
7. Low, X. N., Z. N. Chen, and T. S. P. See, "A UWB dipole antenna with enhanced impedance and gain performance," *IEEE Transactions on Antennas and Propagation*, Vol. 57, No. 10, Oct. 2009.
8. Karakolak, T. and E. Topsakal, "A double-sided rounded bow-tie antenna (DSRBA) for UWB comunication," *IEEE Antennas and Wireless Propagation Letters*, Vol. 5, 2006.
9. Lizzi, L., G. Oliveri, P. Rocca, and A. Massa, "Planer monopole UWB antenna with Unii1/Unii2 WLAN-band notched characteristics," *Progress In Electromagnetics Research B*, Vol. 25, 277–292, 2010.
10. Mushiake, Y., "Self-complementary antennas," *IEEE Antennas and Propagation Magazine*, Vol. 34, No. 6, 23–29, Dec. 1992.
11. Guo, L., X. Chen, and C. Parini, "Study of a miniaturized quasi-self-complementary UWB antenna in frequency and time domain," *Radioengineering*, Vol. 18, No. 4, 381–387, Dec. 2009.
12. Ray, K. P., "Design aspects of printed monopole antennas for UWB applications," *International Journal of Antennas and Propagation*, Vol. 28, 2008.